Electronic Supplementary Material (ESI) for Physical Chemistry Chemical Physics.
This journal is © the Owner Societies 2015

Electronic Supplementary Information

Two equivalent methyl internal rotations in 2,5-dimethylthiophene investigated by microwave spectroscopy

Vinh Van[*a], *Wolfgang Stahl*[a], *and Ha Vinh Lam Nguyen*[b]

[a] Institute of Physical Chemistry, RWTH Aachen University, Landoltweg 2, D-52074 Aachen, Germany.

[b] Laboratoire Interuniversitaire des Systèmes Atmosphériques (LISA), UMR 7583 (CNRS/ Univ. Paris Est & Paris Diderot), Université Paris Est, 61 avenue du Général de Gaulle, F-94010 Créteil cedex, France.

Corresponding author: Vinh Van

Phone: +49 241 80 94753

Email: vinh.van@rwth-aachen.de

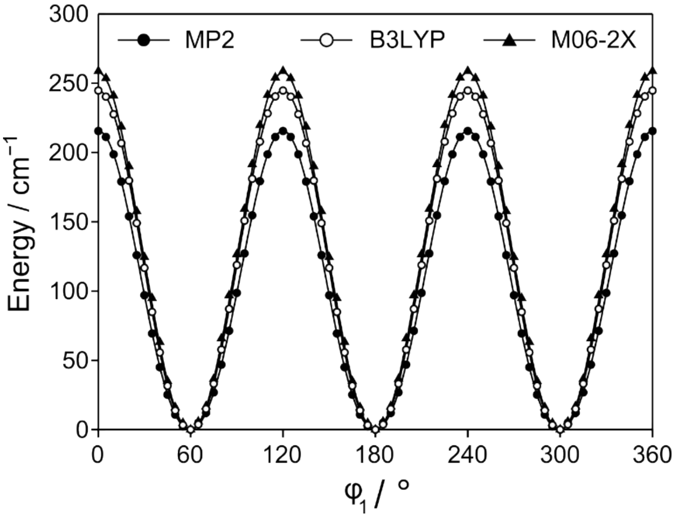

Figure S-F1: The potential energy curves obtained by rotating one methyl group around the C_{12}–C_{10} bond (for atom number see Figure 2). The dihedral angle $\varphi_1 = \angle(S_{15},C_{12},C_{10},H_4)$ was varied in a step width of 1°. The basis set cc-pVTZ was used in combination with the MP2, B3LYP, and M06-2X methods. Relative energies are given with respect to the absolute minima of E = −630.646179 Hartree (MP2), −631.761983 Hartree (B3LYP), and −631.617104 Hartree (M06-2X).

Table S1: Fourier coefficients of the potential energy curves obtained by rotating one methyl group around the C_{12}–C_{10} bond (for atom number see Figure 2). The dihedral angle $\varphi_1 = \angle(S_{15},C_{12},C_{10},H_4)$ was varied in a step width of 1°. Calculations were performed using different methods and the cc-pVTZ basis set (see Figure S-F1). The potential is expanded as

$$V(\varphi) = a_0 + \sum_{n=3}^{15} a_n \cos(n\varphi) + \sum_{n=3}^{9} b_n \sin(n\varphi) .$$

	MP2/ cc-pVTZ		**B3LYP/cc-pVTZ**		**M06-2X/cc-pVTZ**	
	Hartree	cm^{-1}	Hartree	cm^{-1}	Hartree	cm^{-1}
a_0	−630.645711484		−631.761436484		−631.616516796	
a_3	−0.000492240	−108.0	−0.000560540	−123.0	−0.000584515	−128.3
a_6	0.000022517	4.9	0.000010775	2.4	0.000012199	2.7
a_9	0.000000942	0.2	0.000001992	0.4	−0.000004691	−1.0
a_{12}	0.000000497	0.1	0.000000433	0.1	0.000000805	0.2
a_{15}			0.000000981	0.2	0.000001996	0.4

b_3	0.000003408	0.7	0.000004272	0.9	0.000004708	1.0
b_6	0.000001594	0.3	0.000000817	0.2	0.000000948	0.2
b_9					−0.000000584	−0.1

Table S2: Cartesian nuclear coordinates of 2,5-dimethylthiophene calculated at the MP2/ cc-pVTZ level of theory. The atoms are numbered according to Figure 2.

	a /Å	b /Å	c /Å
H1	−3.310351	−0.650870	0.000219
H2	−2.959398	0.834773	−0.880626
H3	−2.959327	0.835141	0.880416
H4	3.310351	−0.650870	−0.000175
H5	2.959385	0.834781	0.880652
H6	2.959341	0.835133	−0.880389
H7	−1.318693	−2.292040	−0.000001
H8	1.318692	−2.292040	−0.000015
C9	−2.697926	0.248923	0.000007
C10	2.697926	0.248923	0.000021
C11	−1.254300	−0.137267	0.000023
C12	1.254300	−0.137268	−0.000015
C13	−0.708113	−1.400395	−0.000003
C14	0.708112	−1.400395	−0.000010
S15	0.000000	1.047653	−0.000011

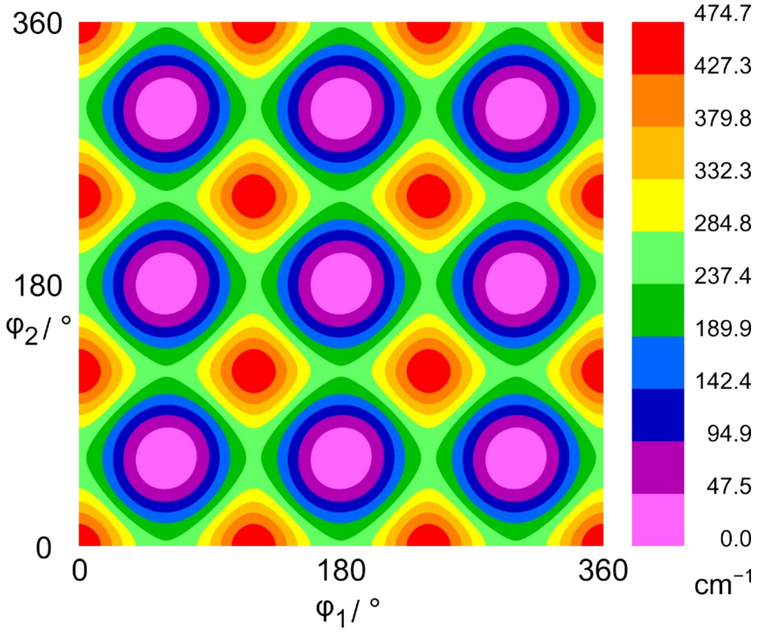

Figure S-F2: The potential energy surface of 2,5-dimethylthiophene calculated at the MP2/6–311++G(d,p) level of theory obtained by rotating the two methyl groups. No significant coupling was observed.

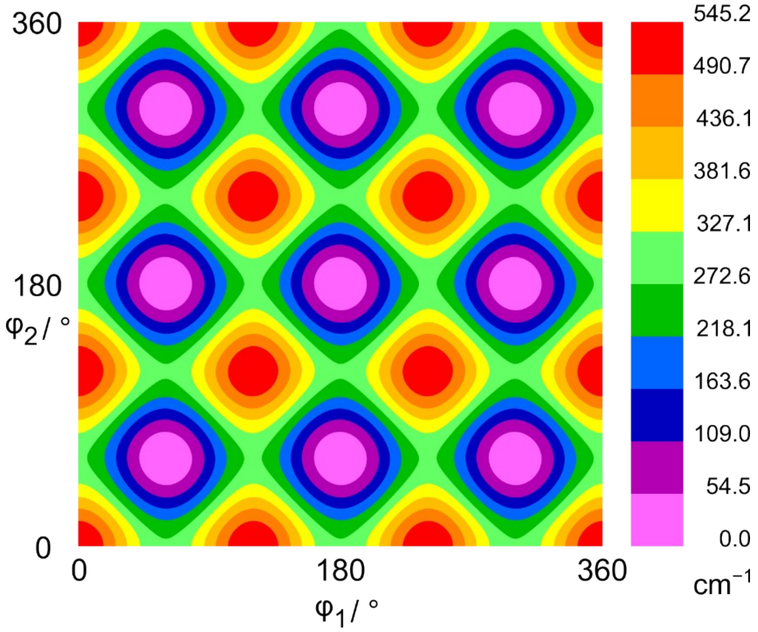

Figure S-F3: The potential energy surface of 2,5-dimethylthiophene calculated at the B3LYP/6–311++G(d,p) level of theory obtained by rotating the two methyl groups. No significant coupling between the torsional motions was observed.

Table S3: Coefficients of the two-dimensional Fourier expansion for the potential energy surface calculated at the MP2/6-311++G(d,p) and B3LYP/6-311++G(d,p) level of theory in a grid of 10° (Figure S-F2 and S-F3). Due to symmetry, only data points in the range from φ_1 = 0° to 120° and φ_2 = 0° to 120° are needed. The potential is expanded as $V(\varphi_1,\varphi_2) = \sum_{n=1}^{12} V_i f_i$.

		MP2/6–311++G(d,p)	B3LYP/6–311++G(d,p)
i	f_i	V_i/Hartree	V_i/Hartree
1	1	−630.445037756	−631.729233044
2	$\cos(3\varphi_1) + \sin(3\varphi_2)$	0.000006328	0.000005076
3	$\cos(3\varphi_1) + \cos(3\varphi_2)$	0.000538003	0.000620153
4	$\cos(6\varphi_1) + \sin(6\varphi_2)$	−0.000001196	−0.000001883
5	$\cos(6\varphi_1) + \cos(6\varphi_2)$	0.000054143	0.000015548
6	$\cos(3\varphi_1)\cos(3\varphi_2)$	−0.000010439	−0.000014867
7	$\sin(3\varphi_1)\sin(3\varphi_2)$	−0.000011985	0.000016431
8	$\cos(6\varphi_1)\cos(6\varphi_2)$	0.000002005	
9	$\sin(6\varphi_1)\sin(6\varphi_2)$	−0.000001900	0.000000231
10	$\cos(3\varphi_1)\sin(3\varphi_2) + \sin(3\varphi_1)\cos(3\varphi_2)$	0.000000705	0.000000279
11	$\cos(6\varphi_1)\cos(3\varphi_2) + \cos(3\varphi_1)\cos(6\varphi_2)$	0.000001777	
12	$\sin(6\varphi_1)\sin(3\varphi_2) + \sin(3\varphi_1)\sin(6\varphi_2)$	0.000002986	

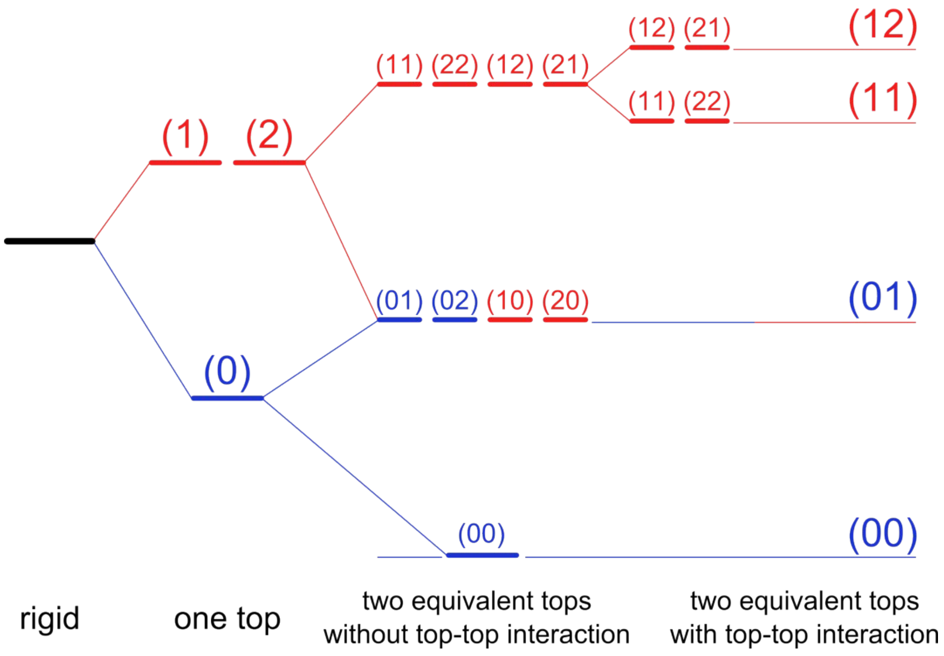

Figure S-F4: Schematic energy level diagram to illustrate the internal rotation splittings. Left-hand side: rigid molecule; middle: splittings to a (0) and an (1) species due to internal rotation of a methyl top; right-hand side: splittings to a (00), a doubly degenerated (01), an (11) and an (12) species due to the internal rotations of two equivalent methyl tops.

Table S4 (next page): The rotational constants *A*, *B*, and *C* in GHz, the deviations (Dev.) between the experimental and calculated rotational constants in MHz, the angles between the internal rotor axis and the principal axes of inertia ∠(i,*a*), ∠(i,*b*), ∠(i,*c*) of the methyl group containing the C_{10} atom, and the barrier to internal rotation V_3 of the two equivalent methyl groups calculated using various methods and basis sets. Additionally, harmonic frequency calculations were carried out to verify the nature of the stationary points.

Method/Basis set	***A***	**Dev.**	***B***	**Dev.**	***C***	**Dev.**	**∠(i,*a*)**	**∠(i,*b*)**	**∠(i,*c*)**	**V_3/cm^{-1}**
HF/6-31G(d,p)	5.024	−59	1.742	5	1.314	−1	14.89	75.11	90.00	382.5
HF/6-31+G(d,p)	5.019	−54	1.740	7	1.313	0	14.97	75.03	90.00	392.3
HF/6-31++G(d,p)	5.019	−54	1.740	7	1.313	0	14.97	75.03	90.00	393.5
HF/6-311G(d,p)	5.029	−64	1.743	4	1.315	−2	14.95	75.05	90.00	380.0
HF/6-311+G(d,p)	5.027	−62	1.742	5	1.314	−1	15.01	74.99	90.00	398.2
HF/6-311++G(d,p)	5.027	−62	1.742	5	1.314	−1	15.01	74.99	90.00	405.2
HF/6-311++G(3df,2pd)	5.077	−112	1.751	−4	1.323	−10	14.93	75.07	90.00	366.2
B3LYP/6-31G(d,p)	4.927	38	1.727	20	1.299	14	14.89	75.11	90.00	294.4
B3LYP/6-31+G(d,p)	4.920	44	1.725	22	1.298	16	14.96	75.04	90.00	292.9
B3LYP/6-31++G(d,p)	4.921	44	1.725	22	1.298	16	14.95	75.05	90.00	290.8
B3LYP/6-311G(d,p)	4.940	25	1.731	16	1.302	11	14.92	75.08	90.00	271.0
B3LYP/6-311+G(d,p)	4.940	25	1.730	17	1.302	11	14.98	75.02	90.00	275.4
B3LYP/6-311++G(d,p)	4.940	25	1.730	17	1.302	11	14.98	75.02	90.00	279.1
B3LYP/6-311++G(3df,2pd)	4.998	−33	1.741	6	1.312	1	14.88	75.12	90.00	230.7
B3LYP/cc-pVDZ	4.900	65	1.723	24	1.296	18	15.01	74.99	90.00	270.6
B3LYP/cc-pVTZ	4.979	−14	1.738	9	1.309	4	14.89	75.11	90.00	244.6
B3LYP/cc-pVQZ	4.991	−26	1.741	6	1.311	2	14.90	75.10	90.00	237.7
M06-2X/6-31G(d,p)	4.967	−2	1.745	1	1.313	1	15.06	74.94	90.00	298.8
M06-2X/6-31+G(d,p)	4.961	4	1.744	3	1.311	2	15.13	74.87	89.99	296.1
M06-2X/6-31++G(d,p)	4.962	3	1.744	3	1.311	2	15.12	74.88	89.99	295.2
M06-2X/6-311G(d,p)	4.977	−12	1.748	−1	1.315	−2	15.09	74.91	90.00	282.6
M06-2X/6-311+G(d,p)	4.977	−12	1.747	0	1.314	−1	15.16	74.84	90.00	290.5
M06-2X/6-311++G(d,p)	4.977	−12	1.747	0	1.314	−1	15.16	74.84	90.00	295.2
M06-2X/6-311++G(3df,2pd)	5.027	−62	1.756	−10	1.323	−10	15.09	74.91	90.00	255.2
M06-2X/cc-pVDZ	4.946	19	1.742	5	1.310	4	15.18	74.82	90.00	281.8
M06-2X/cc-pVTZ	5.014	−49	1.754	−7	1.321	−8	15.07	74.93	90.00	261.6
M06-2X/cc-pVQZ	5.026	−61	1.757	−10	1.323	−10	15.09	74.91	89.99	253.6
MP2/6-31G(d,p)	4.952	13	1.746	1	1.312	1	14.72	75.28	90.00	247.4
MP2/6-31+G(d,p)	4.941	24	1.744	3	1.310	4	14.85	75.18	89.17	
MP2/6-31++G(d,p)	4.941	24	1.744	3	1.310	4	14.87	75.16	89.06	
MP2/6-311G(d,p)	4.943	22	1.745	2	1.311	3	14.82	75.18	90.00	248.4

MP2/6-311+G(d,p)	4.941	24	1.743	4	1.309	4	14.86	75.14	90.00	238.9
MP2/6-311++G(d,p)[a]	4.941	24	1.742	4	1.309	4	14.90	75.10	89.96	241.2
MP2/cc-pVDZ	4.877	88	1.728	19	1.297	17	15.03	74.97	90.00	245.2
MP2/cc-pVTZ	4.980	−15	1.752	−5	1.317	−4	14.98	75.02	90.00	215.5
MP2/cc-pVQZ	5.006	−41	1.758	−11	1.322	−9	15.03	74.97	90.00	
CCSD/6-311++G(d,p)	4.924	41	1.733	14	1.303	10	14.97	75.03	90.00	
CCSD/cc-pVDZ	4.858	107	1.719	28	1.290	23	15.07	74.93	90.00	
CCSD(T)/cc-pVTZ[b]	4.980	−15	1.752	−5	1.317	−4	14.98	75.02	90.00	275.0
Experiment	**4.965**		**1.747**		**1.313**		**14.59**	**75.41**	**90.0**	**248.0**

[a] One imaginary frequency was obtained for the minimum structure (see text) [b] Single point calculations using the optimized structures calculated at the MP2/cc-pVTZ level.

Table S5: Observed frequencies ($\nu_{\mathrm{Obs.}}$) of the (00), (01), (11), and (12) torsional species of 2,5-dimethylthiophene. $\nu_{\mathrm{Obs.}} - \nu_{\mathrm{Calc.}}$ values as obtained after a fit with the program XIAM.

J	K_a	K_c	J	K_a	K_c		$\nu_{\mathrm{Obs.}}$	$\nu_{\mathrm{Obs.}} - \nu_{\mathrm{Calc.}}$
upper level			lower level				GHz	kHz
2	2	1	2	1	2	(00)	10.9765365	−2.3
						(01)	10.7878122	6.4
						(12)	10.5955690	−1.8
						(11)	10.9440246	−0.5
3	1	3	2	0	2	(00)	11.3387590	1.4
						(01)	11.3295459	0.5
						(12)	11.3126677	0.3
						(11)	11.3281475	−0.1
3	2	1	3	1	2	(00)	9.2541060	0.6
						(01)	9.3559650	4.1
						(12)	9.5148455	0.9
						(11)	9.2224300	0.0
3	2	2	2	1	1	(00)	18.8568018	−6.8
						(01)	18.7112833	1.6
						(12)	18.4867022	−0.3
						(11)	18.8240931	0.2
3	2	2	3	1	3	(00)	11.6513380	2.3
						(01)	11.5173545	3.2
						(12)	11.3265087	−1.3
						(11)	11.6187890	−0.4
4	0	4	3	1	3	(00)	9.5343173	−0.2
						(01)	9.5423794	−0.1
						(12)	9.5579888	0.3
						(11)	9.5427464	−0.1
4	1	4	3	0	3	(00)	13.6180181	−0.2
						(01)	13.6105325	0.3
						(12)	13.5983489	0.2
						(11)	13.6078216	0.3
4	2	2	4	1	3	(00)	8.8326193	−4.4
						(01)	8.8742012	−2.6
						(12)	8.9877496	0.2
						(11)	8.8024198	0.1
4	2	3	4	1	4	(00)	12.5615812	1.1
						(01)	12.4886107	2.7
						(12)	12.3438966	−0.4
						(11)	12.5289805	−0.1
4	3	1	3	2	2	(11)	29.5137418	0.3
4	3	1	4	2	2	(00)	16.7680988	−10.1
						(01)	16.9710250	6.1
						(12)	17.1047684	0.0
						(11)	16.7130308	−0.3

4	3	2	3	2	1	(00)	29.3489770	2.1
						(11)	29.2943697	−0.1
4	3	2	4	2	3	(00)	17.3413095	0.7
						(01)	17.0838880	−5.8
						(12)	16.8956150	−0.9
						(11)	17.2877417	0.3
4	4	0	3	3	0	(12)	36.4610260	−1.0
4	4	0	3	3	1	(11)	36.2672629	−0.1
4	4	1	3	3	0	(00)	36.3402495	3.7
						(11)	36.2647106	−1.1
4	4	1	3	3	1	(00)	36.3427845	121.4[a]
						(01)	36.2059699	1.5
						(12)	36.0707866	0.8
5	0	5	4	1	4	(00)	12.8104635	−0.2
						(01)	12.8161123	−0.3
						(12)	12.8261327	0.2
						(11)	12.8173160	0.0
5	1	5	4	0	4	(00)	15.8274913	0.3
						(01)	15.8211763	0.3
						(12)	15.8117354	0.0
						(11)	15.8180447	0.3
5	2	3	5	1	4	(00)	8.5883523	0.6
						(01)	8.6002029	−0.2
						(12)	8.6573483	−0.2
						(11)	8.5606005	0.0
5	2	4	5	1	5	(00)	13.7100406	0.2
						(01)	13.6680106	−2.1
						(12)	13.5809972	0.1
						(11)	13.6773378	0.0
5	3	2	5	2	3	(00)	16.3000706	1.1
						(01)	16.5097668	3.6
						(12)	16.7006530	−2.1
						(11)	16.2441595	0.6
5	3	3	5	2	4	(00)	17.5487510	1.0
						(01)	17.2843342	1.1
						(12)	17.0385646	0.9
						(11)	17.4957106	−0.8
5	4	1	4	3	1	(01)	39.4707114	−1.7
						(12)	39.5305356	−1.4
5	4	1	4	3	2	(00)	39.4198024	−1.5
						(11)	39.3442656	−0.3
5	4	2	4	3	1	(00)	39.4019011	−2.3
						(11)	39.3262585	1.4
5	4	2	4	3	2	(01)	39.2752427	1.2
						(12)	39.1398133	−0.9

6	0	6	5	1	5	(00)	15.9609636	−0.3
						(01)	15.9648206	−0.7
						(12)	15.9713286	0.2
						(11)	15.9659788	0.4
6	1	5	5	2	4	(00)	11.9941358	−0.2
						(01)	12.0369669	0.9
						(12)	12.1303855	0.5
						(11)	12.0228012	−0.5
6	1	5	6	0	6	(00)	9.7432119	−0.6
						(01)	9.7401571	−0.3
						(11)	9.7341613	0.2
6	1	6	5	0	5	(00)	18.0476297	−0.3
						(01)	18.0423861	0.2
						(12)	18.0350255	0.3
						(11)	18.0393073	1.0
6	2	4	6	1	5	(00)	8.6453315	−0.4
						(01)	8.6459070	0.0
						(12)	8.6710172	−0.4
						(11)	8.6209081	0.3
6	2	5	6	1	6	(00)	15.0938338	−0.8
						(01)	15.0647072	−0.6
						(12)	15.0114780	0.2
						(11)	15.0609230	−0.2
6	3	3	6	2	4	(00)	15.6310127	1.1
						(01)	15.8006644	1.0
						(12)	16.0169060	−1.8
						(11)	15.5746017	1.2
6	3	4	6	2	5	(00)	17.8945907	1.3
						(01)	17.6703043	1.4
						(11)	17.8423639	−0.2
7	0	7	6	1	6	(00)	18.9719345	0.1
						(01)	18.9743628	0.5
						(12)	18.9784023	0.3
						(11)	18.9751414	−0.6
7	1	6	6	2	5	(00)	16.0695913	0.3
						(01)	16.0975961	−0.9
						(11)	16.0959109	0.0
7	1	6	7	0	7	(00)	12.1914914	0.3
						(01)	12.1879419	−0.7
						(12)	12.1871051	1.3
						(11)	12.1816922	0.1
7	1	7	6	0	6	(00)	20.3353917	0.2
						(01)	20.3311854	−0.2
						(12)	20.3255799	−0.6
						(11)	20.3284180	−1.1

7	2	5	7	1	6	(00)	9.1018196	0.0
						(01)	9.0986020	0.2
						(12)	9.1092128	−0.3
						(11)	9.0813360	0.9
7	2	6	6	1	5	(00)	27.2946495	−1.9
						(01)	27.2700520	0.9
						(12)	27.2279202	1.5
						(11)	27.2634222	−1.5
7	2	6	7	1	7	(00)	16.7024726	0.2
						(01)	16.6790225	−0.3
						(12)	16.6423931	1.3
						(11)	16.6691639	−1.8
7	3	4	7	2	5	(00)	14.8294534	0.0
						(01)	14.9308278	−1.3
						(11)	14.7736285	−0.1
7	3	5	6	2	4	(00)	37.0634786	1.3
						(01)	36.8830885	1.5
7	3	5	7	2	6	(00)	18.4141567	−1.0
						(01)	18.2589415	−1.5
						(11)	18.3630346	0.7
7	5	2	7	4	3	(00)	30.7867789	2.3
						(01)	30.8452546	1.3
						(12)	30.8942989	0.8
						(11)	30.6900419	−2.3
7	5	3	7	4	4	(00)	30.8056399	−2.2
						(12)	30.5045854	−0.5
						(11)	30.7090747	1.4

[a] Not included in the fit

Table S6: Comparison of the fits using Watson’s A and Watson’s S reduction in I^r representation using the program XIAM. The centrifugal distortion constants calculated at the MP2/6-311++G(d,p) level of theory are in reasonable agreement with the experimental values in both cases.

a) Watson’s A reduction

Par.[a]	Unit	Fit I	Fit II	Calc.
A	GHz	4.97224360(42)	4.96500697(89)	4.9414
B	GHz	1.74696506(27)	1.74694756(13)	1.7426
C	GHz	1.31337981(20)	1.313336623(81)	1.3094
Δ_J	kHz	0.0684(28)	0.0672(11)	0.0630
Δ_{JK}	kHz	0.2071(93)	0.1579(37)	0.171
Δ_K	kHz	3.2158(98)	0.9161(43)	0.803
δ_J	kHz	0.0196(14)	0.01839(51)	0.0171
δ_K	kHz	0.136(23)	0.1031(89)	0.0390
V_3	cm^{-1}		247.95594(30)	241.2
I_α	uÅ^2		3.16442(39)	
∠(i,a)	°		14.5931(78)[b]	14.90
∠(i,b)	°		75.4069(78)	75.10
∠(i,c)	°		90.00(fixed)	89.96
F_{12}	GHz		−7.320(12)	
D_{pi2J}	kHz		−2.78(25)	
D_{pi2K}	kHz		−98.9(42)	
D_{pi2-}	kHz		1.97(19)	
σ[c]	kHz	2.6	1.9	
N[d]		41	157	

Fit I: Correlation matrix of fitted linear combinations as given in the XIAM output.

B_-	1.000							
B_K	−0.135	1.000						
B_J	0.293	−0.375	1.000					
Δ_J	0.441	−0.377	0.909	1.000				
Δ_K	0.237	−0.096	0.265	0.350	1.000			
Δ_{JK}	−0.332	0.756	−0.390	−0.524	−0.635	1.000		
δ_J	0.942	−0.154	0.296	0.391	0.220	−0.285	1.000	
δ_K	0.430	0.003	0.096	0.381	0.192	−0.321	0.185	1.000

Strongest correlation between δ_J and B_- (0.9422)

b) Watson’s S reduction

Par.[a]	Unit	Fit I	Fit II	MP2/6-311++G(d,p)
A	GHz	4.97224362(42)	4.96500700(89)	4.9414
B	GHz	1.74696478(26)	1.74694735(13)	1.7426
C	GHz	1.31338008(20)	1.313336823(81)	1.3094
D_J	kHz	0.0642(26)	0.06390(97)	0.0618
D_{JK}	kHz	0.2328(89)	0.1774(35)	0.178
D_K	kHz	3.1944(97)	0.8998(43)	0.797
d_1	kHz	−0.0196(14)	−0.01839(51)	−0.0171
d_2	kHz	−0.00214(23)	−0.00163(14)	−0.000619
V_3	cm^{-1}		247.95610(30)	241.2
I_α	uÅ^2		3.16442(39)	
∠(i,a)	°		14.5931(78)[b]	14.90
∠(i,b)	°		75.4069(78)	75.10
∠(i,c)	°		90.00(fixed)	89.96
F_{12}	GHz		−7.320(12)	
D_{pi2J}	kHz		−2.77(25)	
D_{pi2K}	kHz		−99.0(42)	
D_{pi2-}	kHz		1.97(19)	

σ^c	kHz	2.6	1.9
N^d		41	157

Fit I: Correlation matrix of fitted linear combinations as given in the XIAM output.

B_-	1.000	
B_K	−0.148	1.000

Fit II, Watson's A: Correlation matrix of fitted linear combinations as given in the XIAM output.

B_-	1														
B_K	−0.078	1													
B_J	0.456	−0.048	1												
Δ_J	0.385	0.029	0.75	1											
Δ_K	0.231	0.411	0.267	0.342	1										
Δ_{JK}	−0.287	0.015	−0.310	−0.501	−0.624	1									
δ_J	0.793	0.082	0.299	0.433	0.24	−0.275	1								
δ_K	0.222	0.169	−0.025	0.376	0.195	−0.309	0.181	1							
V_{1n}	0.142	0.896	0.173	0.061	0.462	−0.101	0.102	0.056	1						
delta	−0.477	0.137	−0.415	0.031	−0.107	0.041	−0.006	0.251	−0.294	1					
F_0	0.098	0.932	0.136	0.066	0.463	−0.099	0.104	0.083	0.995	−0.201	1				
F_{12}	0.009	0.066	−0.015	0.072	−0.004	−0.019	0.048	0.122	0.039	0.043	0.043	1			
$D_{\mathrm{pi}2K}$	0.066	−0.992	0.012	−0.077	−0.426	0.081	−0.101	−0.172	−0.903	−0.140	−0.939	−0.065	1		
$D_{\mathrm{pi}2J}$	−0.415	0.051	−0.599	−0.041	−0.101	0.013	−0.061	0.172	−0.268	0.719	−0.203	0.062	−0.055	1	
$D_{\mathrm{pi}2-}$	−0.539	0.034	−0.410	0.007	−0.151	0.063	−0.014	0.194	−0.345	0.878	−0.265	0.068	−0.035	0.702	1

strongest correlation between F_0 and V_{1n} (0.9953)

Fit II, Watson's S: Correlation matrix of fitted linear combinations as given in the XIAM output.

B_-	1												
B_K	−0.128	1											
B_J	0.475	−0.048	1										
D_J	0.325	−0.017	0.81	1									
D_{JK}	0.202	0.359	0.279	0.277	1								
D_K	−0.241	0.097	−0.334	−0.410	−0.612	1							
d_1	−0.759	−0.083	−0.297	−0.411	−0.183	0.198	1						
d_2	0.057	−0.171	0.032	−0.113	0.133	−0.161	0.182	1					
V_{1n}	0.13	0.895	0.174	0.049	0.449	−0.078	−0.102	−0.056	1				
delta	−0.560	0.137	−0.418	−0.040	−0.191	0.163	0.006	−0.251	−0.296	1			
F_0	0.078	0.932	0.136	0.047	0.441	−0.063	−0.104	−0.083	0.995	−0.202	1		
F_{12}	−0.026	0.066	−0.015	0.042	−0.044	0.039	−0.048	−0.122	0.039	0.042	0.043	1	
$D_{\mathrm{pi}2K}$	0.116	−0.992	0.013	−0.033	−0.374	0.001	0.101	0.172	−0.902	−0.139	−0.939	−0.065	1

B_J	0.288	−0.374	1.000					
D_J	0.343	−0.403	0.948	1.000				
D_{JK}	0.149	−0.101	0.232	0.276	1.000			
D_K	−0.205	0.793	−0.362	−0.431	−0.626	1.000		
d_1	−0.971	0.151	−0.294	−0.368	−0.153	0.209	1.000	
d_2	−0.122	−0.019	−0.089	−0.129	0.174	−0.144	0.185	1.000

Strongest correlation between d_1 and B_- (−0.9711)

D_{pi2J}	−0.474	0.051	−0.600	−0.093	−0.160	0.097	0.06	−0.173	−0.269	0.72	−0.203	0.062	−0.055	1	
D_{pi2-}	−0.607	0.034	−0.411	−0.048	−0.217	0.159	0.014	−0.194	−0.346	0.878	−0.266	0.068	−0.034	0.703	1

strongest correlation between F_0 and V_{1n} (0.9953)